# Communication: Molecular-level insights into asymmetric triblock copolymers: Network and phase development

Syamal S. Tallury, Kenneth P. Mineart, Sebastian Woloszczuk, David N. Williams, Russell B. Thompson, Melissa A. Pasquinelli, Michal Banaszak, and Richard J. Spontak

Citation: The Journal of Chemical Physics **141**, 121103 (2014); doi: 10.1063/1.4896612
View online: http://dx.doi.org/10.1063/1.4896612
View Table of Contents: http://scitation.aip.org/content/aip/journal/jcp/141/12?ver=pdfcov
Published by the AIP Publishing



# Communication: Molecular-level insights into asymmetric triblock copolymers: Network and phase development

Syamal S. Tallury,[1,2] Kenneth P. Mineart,[3] Sebastian Woloszczuk,[4] David N. Williams,[3] Russell B. Thompson,[5] Melissa A. Pasquinelli,[2] Michal Banaszak,[4,a)] and Richard J. Spontak[1,3,a)]

[1]*Department of Materials Science and Engineering, North Carolina State University, Raleigh, North Carolina 27695, USA*
[2]*Fiber and Polymer Science Program, North Carolina State University, Raleigh, North Carolina 27695, USA*
[3]*Department of Chemical and Biomolecular Engineering, North Carolina State University, Raleigh, North Carolina 27695, USA*
[4]*Faculty of Physics, Adam Mickiewicz University, 61-614 Poznan, Poland*
[5]*Department of Physics and Astronomy and Waterloo Institute for Nanotechnology, University of Waterloo, Waterloo, Ontario N2L 3G1, Canada*

(Received 16 August 2014; accepted 16 September 2014; published online 29 September 2014; publisher error corrected 1 October 2014)

Molecularly asymmetric triblock copolymers progressively grown from a parent diblock copolymer can be used to elucidate the phase and property transformation from diblock to network-forming triblock copolymer. In this study, we use several theoretical formalisms and simulation methods to examine the molecular-level characteristics accompanying this transformation, and show that reported macroscopic-level transitions correspond to the onset of an equilibrium network. Midblock conformational fractions and copolymer morphologies are provided as functions of copolymer composition and temperature. © *2014 AIP Publishing LLC*. [http://dx.doi.org/10.1063/1.4896612]

Block copolymers remain one of the most extensively studied genres of macromolecules to date due to their intrinsic ability to (i) self-organize spontaneously into a wide variety of periodic nanostructures[1,2] and (ii) compatibilize immiscible polymers,[3,4] as well as stabilize polymer nanolaminates,[5,6] by locating at polymer/polymer interfaces. These intriguing soft materials can likewise form molecular and supramolecular networks upon microphase separation. Molecular networks develop in multiblock copolymers possessing at least one midblock capable of spanning between, and physically connecting, neighboring microdomains, whereas supramolecular networks are nanostructural motifs that can be described as connected microdomain channels,[7–9] which frequently yield bicontinuous morphologies.[10] In this study, we only consider molecular networks created by microphase-ordered ABA triblock copolymers with glassy endblocks and a rubbery midblock (generically regarded as thermoplastic elastomers.[11]) Due to their highly elastic molecular network, ABA copolymer systems are ubiquitous in a wide range of contemporary technologies requiring, for example, highly stretchable wires for flexible electronics,[12] nanostructured membranes for fuel cells,[13] micromolded substrates for microfluidics,[14] high permittivity nanocomposites for sensors,[15] and energy-efficient dielectric elastomers for actuators and energy-harvesting media.[16–18] Here, we seek to follow the transition from diblock copolymers, a soft materials archetype responsible for elucidating the mechanism of molecular self assembly, to triblock copolymers, another soft materials archetype in which molecular architecture enables network formation and imparts valuable macroscopic properties.

Independent experimental[19,20] and theoretical[21–23] investigations have long sought to correlate the fraction of midblock bridging with bulk mechanical properties in molecularly symmetric copolymers (with A-endblocks of equal repeat unit number, $N_A$) in the melt, as well as in the presence of a selective solvent.[24] In this case, each copolymer molecule can be classified as either a bridge (each endblock resides in a different microdomain), a loop (both endblocks locate within the same microdomain), a dangle (one endblock sits in a microdomain while the other remains in the matrix), or mixed (both endblocks are unsegregated and stay within the matrix). The classifications arising from microphase-segregated chains are depicted in Fig. 1(a). To explore the transition from an AB diblock copolymer with a B tail tethered at a single junction to an ABA triblock copolymer with a B midblock tethered at both ends (to form a bridge or loop), Hamersky *et al.*[25] have examined the phase behavior of $A_1BA_2$ triblock copolymers custom-synthesized from parent diblock copolymers so that $N_{A1} \neq N_{A2}$. Their results reveal that the order-disorder transition temperature ($T_{ODT}$) first decreases as the $A_2$ block is initially grown and then increases upon further progression. Although several theoretical models have been proposed[26–28] to explain the phase behavior of $A_1BA_2$ copolymers, the Mayes-Olvera de la Cruz (MOC) theory,[26] which extends earlier fluctuation theory,[29] has been successfully used, along with on-lattice Monte Carlo (MC) simulations,[30] to quantitatively predict this unexpected observation.

To relate molecular asymmetry to the distribution of A segments in the endblocks, we define $\tau$ as $N_{A1}/(N_{A1} + N_{A2})$

a)Authors to whom correspondence should be addressed. Electronic addresses: mbanasz@amu.edu.pl and rich_spontak@ncsu.edu.

 

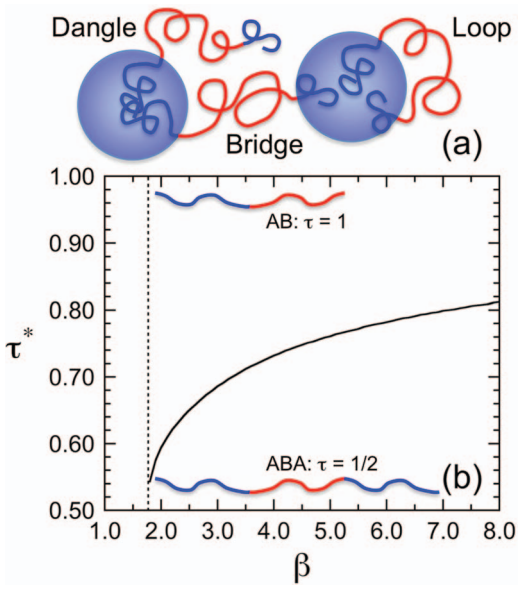


FIG. 1. (a) Schematic illustration of triblock copolymer micelles depicting bridges, loops, and dangles (labeled). (b) Values of $\tau^*$ evaluated from the MOC theory[26] as the value of $\tau$ corresponding to the predicted minimum in $T_{ODT}$ (or, alternatively, the maximum in $\chi N$ at the order-disorder transition), and presented as a function of the parent diblock composition ($\beta$). The dotted vertical line identifies the point below which $\tau^*$ is no longer observed. The depicted molecules correspond to $\tau = 1$ and $\tau = 1/2$ (labeled).

and $\tau^*$ as the asymmetry corresponding to the minimum in $T_{ODT}$. While variation in $\tau$ also promotes differences in copolymer nanostructure and bulk properties,[31,32] changes in midblock bridging with $\tau$ have only been indirectly inferred thus far. In this work, the MOC theory and self-consistent field theory (SCFT) are used in concert with both MC and dissipative particle dynamics (DPD) simulation methods to (i) discern the molecular origin of $\tau^*$, as well as fundamental relationships between $\tau$, midblock conformations, and morphology, and (ii) transcend earlier studies devoted exclusively to either diblock or triblock copolymers by establishing a molecular-level connection between these two important soft material archetypes.

Details of the MOC theory are provided in Ref. 26, whereas the SCFT employed here is based on the framework developed[22] to predict the bridging fraction in molecularly symmetric $A_1BA_2$ triblock copolymers with $N_{A1} = N_{A2}$ ($\tau = 1/2$). While DPD simulations have also focused on such copolymers,[33–35] we extend such simulations to molecularly asymmetric triblock systems varying in $\tau$ and containing 1000 molecules ranging in length up to 224 connected beads (each bead is ~0.33 kDa) by using the parameterization described in Ref. 36 and the Large-scale Atomic/Molecular Massively Parallel Simulator (LAMMPS) software suite.[37] The interaction energy between segments $i$ and $j$ ($i,j$ = A or B) is designated as $\varepsilon_{ij}$ with $\varepsilon_{AA} = \varepsilon_{BB} = 25kT$ and $\varepsilon_{AB}$ varying from 35kT to 50kT, where k is the Boltzmann constant and T denotes absolute temperature.[38,39] After equilibration at 100 °C, we differentiate chain classifications by identifying how beads contribute to the copolymer morphology according to a density-based shape-recognition algorithm,[36] thereby avoiding oversimplifying assumptions due to strong segregation. The MC simulations utilize a cooperative motion algorithm performed on a face-centered cubic lattice, as detailed earlier.[30] The simulation box size is chosen to fit the copolymer chain, and all lattice sites within the box are completely filled with chain segments (each ~1 kDa) so that the movement of one segment necessitates cooperative motion of other segments. Pairwise interaction energies are given by $\varepsilon_{AA} = \varepsilon_{BB} = 0$ and $\varepsilon_{AB} = \varepsilon = \chi kT/(z-2)$, where $\chi$ is the Flory-Huggins parameter and z (=12) is the coordination number. Each simulation is equilibrated at $T^*$ (=$kT/\varepsilon$), and parallel tempering[40] overcomes local free energy minima at low T and long relaxation times.

The observed[25] minimum in $T_{ODT}$ at $\tau^*$ as $N_{A2}$ is increased (and $\tau$ decreases from unity) can be interpreted in terms of a dilution effect: short $A_2$ endblocks are insufficiently incompatible with B midblocks to microphase-separate and remain mixed in the midblock-rich matrix. Inclusion of $A_2$ endblocks in the matrix serves to reduce the effective thermodynamic incompatibility of the copolymer and, hence, $T_{ODT}$. When the $A_2$ endblocks are long enough, they microphase-separate along with the $A_1$ blocks as the incompatibility between A and B blocks (and $T_{ODT}$) increases. This trend is evident in Figure 1(b), which displays predictions of $\tau^*$ from the MOC theory as a function of the chemical composition of the parent AB copolymer (expressed as $\beta = N_B/N_{A1}$). An increase in $\beta$ translates into higher copolymer incompatibility under isothermal conditions if $N_{A1}$ is held constant. For copolymers with styrenic endblocks and an isoprenic midblock, $\tau^*$ exhibits a lower limit at $\beta \approx 1.8$, below which $\tau^*$ cannot be discerned. To relate these predictions to chain classifications (i.e., midblock bridges, loops, and dangles), we seek to discern the molecular origin of $\tau^*$. Following the concept proposed by Matsen,[28] the initial reduction in $T_{ODT}$ with decreasing $\tau$ can be attributed to short $A_2$ blocks remaining mixed as dangles within the B matrix due to a low enthalpic penalty relative to the associated entropic gain. As the $A_2$ block is grown, a critical block mass is reached at which the enthalpic penalty promotes microphase separation of the $A_2$ blocks and, thus, co-location of the $A_1$ and $A_2$ blocks with few remaining dangles. In this view, $\tau^*$ corresponds to the transition at which each B midblock transforms into a bridge or loop.

To develop a molecular-level picture of how this transition proceeds, we have conducted DPD simulations on a styrene-isoprene copolymer with a 9 kDa $A_1$-block and a 45 kDa B-block (referred to as 9-45-$A_2$) to match an experimental system reported earlier.[25] Simulation results are analyzed[36] to discern how the fractions of bridges ($f_B$), loops ($f_L$), and dangles ($f_D$) vary with $\tau$. [Since unsegregated chains consistently account for only 2%–3% of the chain populations, they are included in $f_D$ to avoid confusion, in which case $f_B + f_L + f_D = 1$.] The results presented in Figure 2(a) reveal that $f_B$ and $f_L$ both initially increase, while $f_D$ decreases, with decreasing $\tau$ and then reach plateau levels. Gradual, rather than abrupt, increases in both $f_B$ and $f_L$ due to the initial growth of the $A_2$ endblock indicates that the dispersed A-rich microdomains are surrounded by looped midblocks and loosely connected by bridges to form clusters.[24,41] This picture of microdomain clustering fundamentally differs from the previous idea that midblock bridging occurs only

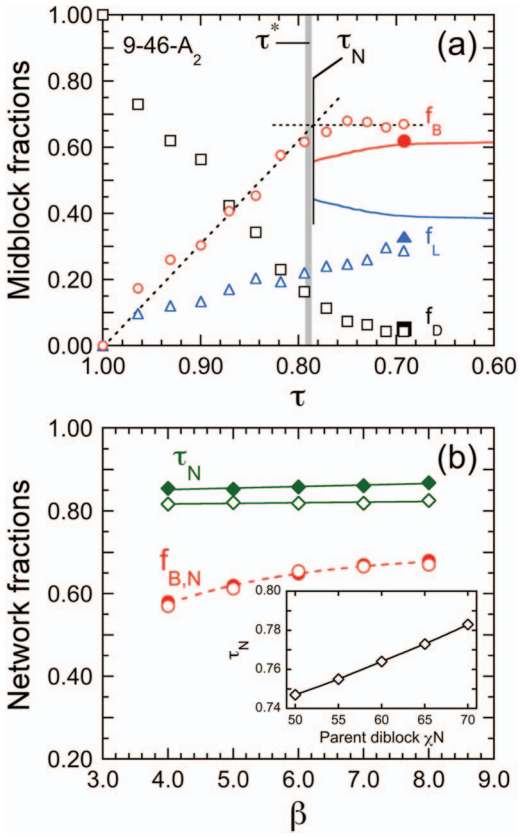


FIG. 2. (a) The dependence of the midblock fractions ($f_B$, red; $f_L$, blue; $f_D$, black) from DPD simulations with $\varepsilon_{AB} = 35kT$ (open symbols), MC simulations (filled symbols), and SCFT predictions (solid lines) on $\tau$ in the 9-46-$A_2$ copolymer series. The intersecting dashed lines yield the value of $\tau_N$, and the gray stripe identifies $\tau^*$ determined from the MOC theory. (b) DPD simulation results of $\tau_N$ (green) and $f_{B,N}$ (red) as functions of $\beta$ for two values of $\varepsilon_{AB}$ (in units of kT): 40 (open symbols) and 50 (filled symbols). The solid lines represent linear regressions of the data, whereas the dashed line serves as a guide for the eye. The variation of $\tau_N$ on parent diblock copolymer incompatibility ($\chi$N) from SCFT is included in the inset, and the solid line is a linear regression.

when a critical $A_2$ block mass is achieved. The transition at which $f_B$ and $f_L$ become independent of $\tau$ is denoted $\tau_N$ and signifies the formation of a fully developed network. At $\tau < \tau_N$, the population of dangles and mixed chains drops below ≈7%, whereas $f_B$ remains nearly constant at ≈0.67. From the intersection of the regressed lines in Figure 2(a), the cluster → network transition is estimated at $\tau_N \approx 0.78$, which coincides with the value of $\tau^*$ (=0.79) obtained by fitting MOC theoretical predictions to discrete experimental data.[25] Such agreement is consistent with the notion that the onset of network formation, and not the onset of molecular bridging, is primarily responsible for the transition from diblock to triblock copolymer behavior.

Figure 2(a) also includes values of $f_B$ and $f_L$ calculated from SCFT (initial parent diblock $\chi N = 70$) for a 9.4-46-$A_2$ copolymer subject to the constraint that $f_B + f_L = 1$ (since $f_D$ cannot be discerned from SCFT). These predictions are extracted from 2D segmental distributions of $A_2$. From $\tau = 0.7$ to $\tau = 0.5$, $f_B$ and $f_L$ remain relatively constant at 0.61 and 0.39, respectively, which agree reasonably well with the DPD simulations considering that the contribution from $f_D$ is omitted. As $\tau$ is increased beyond 0.7, $f_B$ decreases, while $f_L$ increases, slightly until the $A_2$ segmental distributions become sufficiently diffuse to prevent further analysis. In Figure 2(a), this cutoff occurs at $\tau = 0.78$, quantitatively matching both $\tau^*$ and $\tau_N$. At larger values of $\tau$, SCFT is inapplicable due to the non-negligible populations of dangles. A single set of MC simulation results obtained for a 9-45-4 copolymer at $T^* \approx 3$ is provided for comparison in Figure 2(a) to demonstrate further agreement between simulation methods and theory in the network regime. Figure 2(b) displays the variation of $\tau_N$ and the network bridging fraction ($f_{B,N}$) with respect to $\beta$ from DPD simulations performed at two values of $\varepsilon_{AB}$. These findings indicate that, while the values of $\tau_N$ do not change very much with $\beta$, they clearly increase with increasing copolymer incompatibility. This trend is also predicted from SCFT in the inset of Figure 2(b), which shows $\tau_N$ as a function of the parent AB copolymer incompatibility ($\chi$N, where $\chi$ depends on the value of $\varepsilon_{AB}$ used and $N = N_{A1} + N_B$). If the number of repeat units in the parent AB copolymer is constant (as in the 9.4-46-$A_2$ series), then changes in $\chi$N relate to temperature since $\chi \sim 1/T$, thereby establishing that $\tau_N$ depends not only on copolymer composition but also on temperature.

Included in Figure 2(b) are DPD simulation results for the composition dependence of $f_{B,N}$, which appears to be independent of copolymer incompatibility but sensitive to $\beta$. This observation is consistent with the expectation that $f_{B,N}$ decreases as the copolymer becomes increasingly A-rich and the morphology of the system eventually transforms from dispersed A microdomains at relatively high $\beta$ to lamellar in the vicinity of $\beta \approx 1$. As alluded to earlier, morphological transitions are more conventionally induced by changing temperature, which suggests that the reduction in $f_{B,N}$ apparent in Figure 2(b) may alternatively be driven by thermal means. Such dependence is confirmed by the MC simulation results shown in Figure 3 for a 9-45-4 copolymer. At low $T^*$, $f_{B,N}$ varies relatively little (between 0.57 and 0.62) and then decreases significantly (to <0.30) as $T_{ODT}$ is approached. Concurrently, $f_{L,N}$ decreases slightly (from ~0.38 to 0.32) with increasing $T^*$, but then increases close to 0.50 near $T_{ODT}$. Finally, $f_{D,N}$ remains negligibly small (≈0.05) at low $T^*$ and then monotonically increases with increasing $T^*$. These simulation data collectively establish that increasing temperature only slightly affects midblock conformations at conditions far removed from $T_{ODT}$. As transition temperatures are approached, however, $f_{B,N}$ can decrease substantially, and the copolymer network consequently weaken, in favor of increased populations of both loops and dangles. On the basis of these results, we select $T^* = 5.8$ in the following discussion as the highest temperature still sufficiently removed from $T_{ODT}$ to avoid significant changes in the conformational fractions described above.

Thus far, only isomorphic copolymer systems have been discussed in terms of variable $\tau$ or $T^*$. Figure 4 displays the effect of simultaneously varying $\tau$ and either $\beta$ or, more traditionally, $\Phi = N_{A1}/(N_{A1}+N_B) = (1+\beta)^{-1}$ on the phase behavior of $A_1BA_2$ triblock copolymers in the form of an isothermal phase diagram generated from MC simulations. According to visual inspection and Fourier analysis, all of the expected equilibrium morphologies representative

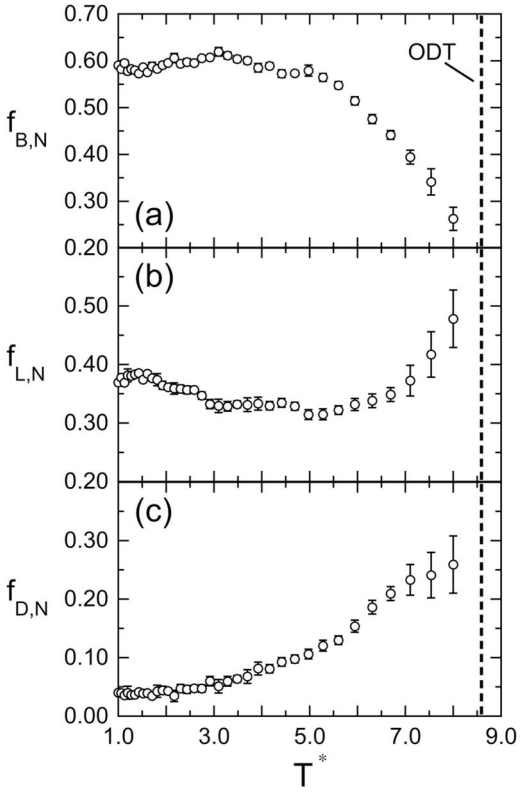


FIG. 3. MC simulation results of the midblock fractions in the network regime— (a) bridge, (b) loop, and (c) dangle — as functions of reduced temperature ($T^*$) for a 9-45-4 copolymer. The ODT is labeled, and the error bars correspond to the standard deviation in the data.

of microphase-ordered AB and ABA copolymers are evident. Isolated regions of perforated lamellae, which are likely to be highly metastable (due to an expected[28] reduction in packing frustration), are also observed. These results confirm that an increase in the length of the $A_2$ block, and a corresponding reduction in $\tau$ from unity, at constant $\beta$ not only introduce

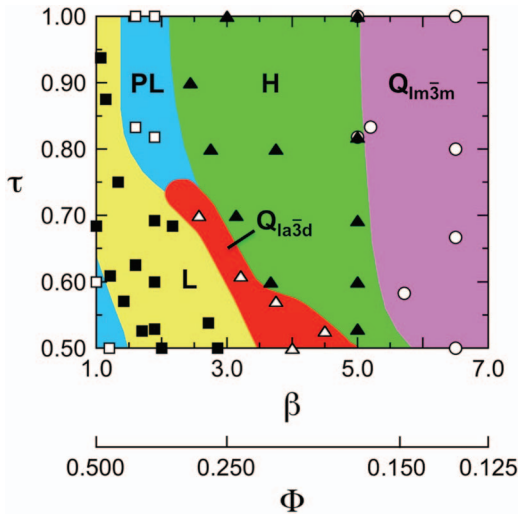


FIG. 4. Isothermal phase diagram along the $\tau$-$\beta$ plane constructed from MC simulations. The morphologies are labeled: lamellae (L), perforated lamellae (PL), gyroid ($Q_{Ia\bar{3}d}$), hexagonally packed cylinders (H), and body-centered-cubic spheres ($Q_{Im\bar{3}m}$). The second abscissa axis converts the $\beta$ scale to the more conventional A-fraction basis ($\Phi$), defined in the text.

midblock bridging but also drive morphological transitions in this class of block copolymers. A change in morphology is, however, accompanied by a change in $f_B$, as discussed earlier (cf. Figure 2). In this spirit, endblock asymmetry can help promote the formation of other organized structures, such as vesicles, in the presence of an endblock-compatible species.[42] When $\tau < \tau_N$ and the $A_2$ blocks predominantly co-locate with the $A_1$ blocks, they form a bidisperse brush insofar as $N_{A1} \neq N_{A2}$. As a single-molecule route[31] to such brushes in confined nanoscale environments, the $A_1BA_2$ design can provide valuable insight into the effect of bidisperse chain packing on interfacial curvature and copolymer phase behavior (cf. Figure 4) without resorting to physical blending. In general, this largely unexplored multiblock copolymer design[43] is helpful in elucidating fundamental relationships between molecular architecture and the evolution of macroscopic properties.

This work was supported by the Nonwovens Institute at North Carolina State University and the Polish Ministry of Science and Higher Education (Grant No. N204 125039). Some SCFT calculations were performed on SHARCNET, whereas the simulations were conducted at the NC State High-Performance Computing Center and the Poznan Supercomputing and Networking Center.

[1] I. W. Hamley, *The Physics of Block Copolymers* (Oxford University Press, New York, 1998).
[2] *Developments in Block Copolymer Science and Technology*, edited by I. W. Hamley (Wiley, New York, 2004).
[3] A. V. Ruzette and L. Leibler, Nat. Mater. **4**, 19 (2005).
[4] Z. Sun, K. Xiao, J. K. Keum, X. Yu, K. L. Hong, J. Browning, I. N. Ivanov, J. H. Chen, J. Alonzo, D. W. Li, B. G. Sumpter, E. A. Payzant, C. M. Rouleau, and D. B. Geohegan, Adv. Mater. **23**, 5529–5535 (2011).
[5] V. Gernigon, P. Leveque, C. Brochon, J. N. Audinot, N. LeClerc, R. Bechara, F. Richard, T. Heiser, and G. Hadziioannou, Eur. Phys. J.: Appl. Phys. **56**, 34107 (2011).
[6] A. O. Gozen, J. J. Zhou, K. E. Roskov, A.-C. Shi, J. Genzer, and R. J. Spontak, Soft Matter **7**, 3268 (2011).
[7] E. W. Cochran and F. S. Bates, Phys. Rev. Lett. **93**, 087802 (2004).
[8] C. A. Tyler and D. C. Morse, Phys. Rev. Lett. **94**, 208302 (2005).
[9] A. J. Meuler, M. A. Hillmyer, and F. S. Bates, Macromolecules **42**, 7221 (2009).
[10] H. Jinnai, Y. Nishikawa, R. J. Spontak, S. D. Smith, D. A. Agard, and T. Hashimoto, Phys. Rev. Lett. **84**, 518 (2000).
[11] G. Holden, H. R. Kricheldorf, and R. P. Quirk, *Thermoplastic Elastomers*, 3rd ed. (Hanser, Munich, 2004).
[12] S. Zhu, J.-H. So, R. Mays, S. Desai, W. R. Barnes, B. Pourdeyhimi, and M. D. Dickey, Adv. Funct. Mater. **23**, 2308 (2013).
[13] Y. A. Elabd and M. A. Hickner, Macromolecules **44**, 1 (2011).
[14] A. P. Sudarsan, J. Wang, and V. M. Ugaz, Anal. Chem. **77**, 5167 (2005).
[15] G. Kofod, S. Risse, H. Stoyanov, D. N. McCarthy, S. Sokolov, and R. Kraehnert, ACS Nano **5**, 1623 (2011).
[16] R. Shankar, T. K. Ghosh, and R. J. Spontak, Adv. Mater. **19**, 2218 (2007).
[17] P. H. Vargantwar, R. Shankar, A. S. Krishnan, T. K. Ghosh, and R. J. Spontak, Soft Matter **7**, 1651 (2011).
[18] B. Kim, Y. D. Park, K. Min, J. H. Lee, S. S. Hwang, S. M. Hong, B. H. Kim, S. O. Kim, and C. M. Koo, Adv. Funct. Mater. **21**, 3242 (2011).
[19] H. Watanabe, T. Sato, K. Osaki, M. L. Yao, and A. Yamagishi, Macromolecules **30**, 5877 (1997); H. Watanabe, T. Sato, and K. Osaki, *ibid.* **33**, 2545 (2000).
[20] L. Kane, D. A. Norman, S. A. White, M. W. Matsen, M. M. Satkowski, S. D. Smith, and R. J. Spontak, Macromol. Rapid Commun. **22**, 281 (2001).
[21] M. W. Matsen and M. Schick, Macromolecules **27**, 187 (1994).
[22] M. W. Matsen and R. B. Thompson, J. Chem. Phys. **111**, 7139 (1999).
[23] M. Banaszak, S. Woloszczuk, T. Pakula, and S. Jurga, Phys. Rev. E **66**, 031804 (2002).

[24]M. Nguyen-Misra and W. L. Mattice, Macromolecules **28**, 1444 (1995).
[25]M. W. Hamersky, S. D. Smith, A. O. Gozen, and R. J. Spontak, Phys. Rev. Lett. **95**, 168306 (2005).
[26]A. M. Mayes and M. Olvera de la Cruz, J. Chem. Phys. **91**, 7228 (1989); **95**, 4670 (1991).
[27]A. V. Dobrynin and I. Ya. Erukhimovich, Macromolecules **26**, 276 (1993).
[28]M. W. Matsen, J. Chem. Phys. **113**, 5539 (2000).
[29]G. H. Fredrickson and E. Helfand, J. Chem. Phys. **87**, 697 (1987).
[30]S. Woloszczuk, M. Banaszak, and R. J. Spontak, J. Polym. Sci. B **51**, 343 (2013).
[31]S. D. Smith, M. W. Hamersky, M. K. Bowman, K. Ø. Rasmussen, and R. J. Spontak, Langmuir **22**, 6465 (2006).
[32]A. O. Gozen, M. K. Gaines, M. W. Hamersky, P. Maniadis, K. Ø. Rasmussen, S. D. Smith, and R. J. Spontak, Polymer **51**, 5304 (2010).
[33]R. D. Groot, T. J. Madden, and D. J. Tildesley, J. Chem. Phys. **110**, 9739 (1999).
[34]C.-I. Huang, H. K. Fang, and C. H. Lin, Phys. Rev. E **77**, 031804 (2008).
[35]Y. R. Sliozberg, J. W. Andzelm, J. K. Brennan, M. R. Vanlandingham, V. Pryamitsyn, and V. Ganesan, J. Polym. Sci. B **48**, 15 (2010).
[36]S. S. Tallury, R. J. Spontak, and M. A. Pasquinelli, "Dissipative particle dynamics of triblock copolymer melts: A midblock conformational study at moderate segregation," J. Chem. Phys. (submitted).
[37]S. Plimpton, J. Comput. Phys. **117**, 1 (1995).
[38]R. D. Groot and T. J. Madden, J. Chem. Phys. **108**, 8713 (1998).
[39]M. A. Horsch, Z. Zhang, C. R. Iacovella, and S. C. Glotzer, J. Chem. Phys. **121**, 11455 (2004).
[40]T. M. Beardsley and M. W. Matsen, Eur. Phys. J. E **32**, 255 (2010).
[41]Č. Koňák, G. Fleischer, Z. Tuzar, and R. Bansil, J. Polym. Sci. B **38**, 1312 (2000).
[42]A. Touris, S. Lee, M. A. Hillmyer, and F. S. Bates, ACS Macro Lett. **1**, 768 (2012).
[43]F. S. Bates, M. A. Hillmyer, T. P. Lodge, C. M. Bates, K. T. Delaney, and G. H. Fredrickson, Science **336**, 434 (2012).